

## Structure and Intramolecular Motions in Triethylenediamine as Studied by Gas Electron Diffraction

Akimichi YOKOZEKI and Kozo KUCHITSU

Department of Chemistry, Faculty of Science, The University of Tokyo, Hongo, Tokyo

(Received August 13, 1970)

The structure and intramolecular motions in triethylenediamine have been investigated by gas electron diffraction with a parallel study of bicyclo[2.2.2]octane in our previous paper. The structural parameters determined by a least-squares analysis on molecular intensities, with estimated limits of error, are as follows:  $r_g(\text{C-N}) = 1.472 \pm 0.007 \text{ \AA}$ ,  $r_g(\text{C-C}) = 1.562 \pm 0.009 \text{ \AA}$ ,  $\angle \text{C-C-N} = 110.2 \pm 0.4^\circ$ ,  $\angle \text{C-N-C} = 108.7 \pm 0.4^\circ$ ,  $r_g(\text{C-H}) = 1.11_0 \pm 0.01_2 \text{ \AA}$  and  $\angle \text{H-C-H} = 111.5 \pm 5.6^\circ$ . The gas-phase structure is in good correspondence with that in the crystal phase determined by Weiss *et al.* by X-ray diffraction. The potential function with regard to the twisting motion around the  $C_3$  symmetry axis is shown to have a broad minimum around the  $D_{3h}$  conformation, being quite analogous to that for bicyclo[2.2.2]octane; in terms of the torsional angle  $\phi$  about the C-C axis, it probably has a small hump of the order of 100 cal/mol at  $\phi = 0^\circ$  and a double minimum around  $\phi = 10^\circ$ . The above study was made with a new nozzle assembly, by which the sample can be heated to about 200°C. The detail of the design and operation is described.

According to our previous study of gas-phase electron diffraction,<sup>1)</sup> bicyclo[2.2.2]octane (hereafter abbreviated as BO) has such a characteristic intramolecular motion with a large amplitude of twisting about the  $C_3$  axis that the molecular symmetry should rightly be called "quasi- $D_{3h}$ ". Since triethylenediamine (TEDA), or 1,4-diazabicyclo[2.2.2]octane (Fig. 1), has an analogous

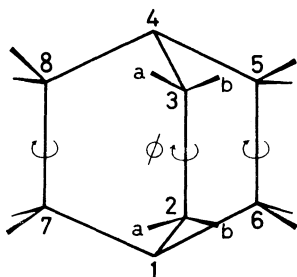


Fig. 1. Triethylenediamine,  $(\text{C}_2\text{H}_4)_3\text{N}_2$ ;  $\phi$  denotes a torsional angle defined by the dihedral angle between the planes  $\text{N}_1\text{-C}_2\text{-C}_3$  and  $\text{C}_2\text{-C}_3\text{-N}_1$ .

skeleton, a similar problem of molecular dynamics is expected for TEDA. In fact, the intramolecular and overall motions in the crystal phase have been investigated by various experimental methods;<sup>2-8)</sup> a particular attention has been paid to the solid-state properties of TEDA, since it belongs to the so-called "plastic crystals."<sup>9,10)</sup>

In spite of such studies, however, the potential function for the twisting motion has not been explored in detail; nor has any conclusion regarding the equilibrium symmetry ( $D_{3h}$  or  $D_3$ ) been reached. Therefore, an electron-diffraction study of gas-phase TEDA was initiated to parallel that of BO. In contrast to the case of BO, where closely-spaced C-C bond distances ( $\text{C}_1\text{-C}_2$  and  $\text{C}_2\text{-C}_3$ ) were hardly separable, the corresponding analysis for TEDA to separate  $\text{N}_1\text{-C}_2$  and  $\text{C}_2\text{-C}_3$  distances poses no serious problem.

In order to get a sufficient vapor pressure, a nozzle assembly, which can be heated to about 200°C, has been constructed. A detail of the design and operation is described in the Appendix.

### Experimental

Anhydrous TEDA (classified as extra pure) was purchased from the Tokyo Chemical Industry Co. Ltd. The sample was loaded in a sample holder (Fig. 3a) in a dry atmosphere. Diffraction photographs were taken on Fuji Process Hard plates with the camera length of 113 mm at the temperature of 120°C (in the sample holder and on the nozzle tip) for 2 min with an apparatus equipped with an  $r^3$ -sector.<sup>11)</sup> The accelerating voltage, about 40 kV, was stabilized within 0.1% during the experiment, and the beam current was 0.40  $\mu\text{A}$ . The scale factor of the diffraction pattern was calibrated to

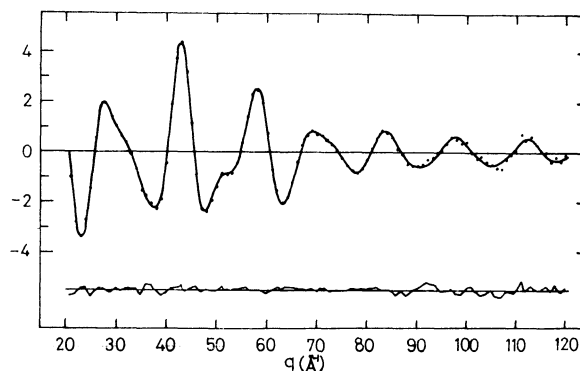


Fig. 2. Experimental (dots) and calculated (upper solid curve) molecular intensity functions for triethylenediamine; the lower curve represents  $[qM(q)_{\text{exp}} - qM(q)_{\text{calc}}]$ .

- 1) A. Yokozeki and K. Kuchitsu, *This Bulletin*, **43**, 2017 (1970).
- 2) P. Brüesch and Hs. H. Günthard, *Spectrochim. Acta*, **22**, 877 (1966).
- 3) M. P. Marzocchi, G. Sbrana, and G. Zerbi, *J. Amer. Chem. Soc.*, **87**, 1429 (1964).
- 4) G. S. Weiss, A. S. Parkes, E. R. Nixon, and R. E. Hughes, *J. Chem. Phys.*, **41**, 3759 (1964).
- 5) T. Wada, E. Kishida, Y. Tomiie, H. Suga, S. Seki, and I. Nitta, *This Bulletin*, **33**, 1317 (1960).
- 6) L. N. Becka, *J. Chem. Phys.*, **38**, 1685 (1963).
- 7) G. W. Smith, *ibid.*, **48**, 4325 (1965).
- 8) A. Zussman and S. Alexander, *ibid.*, **48**, 3534 (1968).
- 9) A. Farkas, G. A. Mills, W. E. Ermer, and J. B. Maerker, *Ind. Eng. Chem.*, **51**, 1299 (1959), *J. Chem. Eng. Data*, **4**, 334 (1959).
- 10) J. C. Trowbridge and E. F. Westrum, Jr., *J. Phys. Chem.*, **67**, 2381 (1963).

within 0.07% with reference to the  $r_a(\text{C-O})$  bond length of carbon dioxide, 1.1646 Å.<sup>11)</sup> and to the  $r_a(\text{N-N})$  distance of the nitrogen gas, 1.1007 Å.<sup>12)</sup> Other experimental and interpretational procedures are similar to those described in Ref. 1. A typical observed molecular intensity<sup>13)</sup> and the difference between the observed and theoretical best-fit curves are shown in Fig. 2.

### Analysis

The analytical procedures closely followed those employed in the study of BO. The mean amplitudes and nonlinear shrinkage corrections<sup>14)</sup> on all the internuclear distances were calculated for a  $D_{3h}$  structure with sets of the Urey-Bradley force constants transferred from those for cyclohexane<sup>15)</sup> and amides.<sup>16)</sup> The vibrational frequencies calculated by the use of the force constants given in Table 1 are in fair agreement with the observed

TABLE 1. UREY-BRADLEY FORCE CONSTANTS FOR TRIETHYLENEDIAMINE<sup>a)</sup> (in md/Å).

$K(\text{C-N})$	5.5	$H(\text{H-C-H})$	0.42
$K(\text{C-C})$	2.3	$F(\text{C}\cdots\text{N})$	0.70
$K(\text{C-H})$	4.3	$F(\text{C}\cdots\text{C})$	0.30
$H(\text{C-C-N})$	0.30	$F(\text{N}\cdots\text{H})$	0.52
$H(\text{C-N-C})$	0.35	$F(\text{C}\cdots\text{H})$	0.41
$H(\text{C-C-H})$	0.225	$F(\text{H}\cdots\text{H})$	0.07
$H(\text{N-C-H})$	0.28	$Y^b)$	(0.11)

a) Estimated from the force constants for cyclohexane,<sup>15)</sup> acetamide and thioamides<sup>16)</sup>

b) See text; in md·Å units.

values reported in the literature,<sup>2-4)</sup> as shown in Table 2. The mean amplitudes and vibrational corrections are insensitive to the moderate changes in the force constants, except for the torsional force constant  $Y$ .<sup>1)</sup> Systematic variations in  $Y$ , 0.11 (estimated upper

limit<sup>1)</sup>), 0.08, 0.05 and 0.025 md·Å, yielded the lowest vibrational frequencies of 137, 118, 94 and 67 cm<sup>-1</sup>, respectively. All the other frequencies were independent of  $Y$ ; this indicates that the normal mode of twisting is separable almost completely from the other modes. The mean amplitudes and vibrational corrections calculated for 120°C are listed in Tables 3 and 4.

**Least-Squares Analysis.** On the assumption that the H-C-H plane is perpendicular to the N-C-C plane and bisects the N-C-C angle and *vice versa*, the molecular intensity ( $q=21$  to 120) was first analyzed by a standard least-squares method<sup>17)</sup> with the sets of constant mean amplitudes and shrinkage corrections, given in Tables 3 and 4, and with the following six variable parameters: the N-C and C-C bond distances, the N-C-C angle, the C-H distance, the H-C-H angle, and the equilib-

TABLE 3. CALCULATED MEAN AMPLITUDES FOR TRIETHYLENEDIAMINE<sup>a)</sup>

$\text{C}_2\text{-N}_1$	442	$\text{N}_1\text{-N}_4$	657	$\text{C}_7\text{-H}_{2b}$	1004
$\text{C}_2\text{-C}_3$	519	C-H	781	$\text{N}_1\text{-H}_7$	1014
$\text{C}_3\text{-N}_1$	602	$\text{C}_2\text{-H}_{3a}$	1069		
Set <sup>b)</sup>	I	II	III	IV	V
$\text{C}_2\text{-C}_7$	695	695	699	704	709
$\text{C}_3\text{-C}_7$	728	877	922	1014	1222
$\text{C}_7\text{-H}_{2a}$	1562	1591	1623	1675	1774
$\text{C}_7\text{-H}_{3a}$	1514	2004	2165	2475	3142
$\text{C}_7\text{-H}_{3b}$	1043	1050	1053	1059	1069
$\text{N}_1\text{-H}_8$	1176	1276	1317	1399	1588

a) Calculated by using the force constants given in Table 1; in 10<sup>-4</sup> units. The hydrogen-hydrogen amplitudes are omitted.

b) Sets I through V correspond to the torsional force constants  $Y$  (see text), assumed to be ∞, 0.11, 0.08, 0.05 and 0.025 md·Å respectively. Values listed in the upper section do not depend on the choice of  $Y$ .

TABLE 2. VIBRATIONAL FREQUENCIES OF TRIETHYLENEDIAMINE

Calcd <sup>a)</sup>	Obsd <sup>b)</sup>	Calcd	Obsd	Calcd	Obsd	Calcd	Obsd
$A_1'$ 2970	2866	$A_1''$ 3001	2920	$E'$ 3017	2950	$E''$ 3003	2930
1465	1447	1222	1243	2971	2866	2985	2882
1309	1335	966	1019	1490	1452	1516	—
1121	965	137 <sup>c)</sup>	—	1442	1316	1446	1447
957	800			1267	1295	1338	—
571	600	$A_2''$ 2984	2882	1203	1061	1210	—
		1457	1460	995	891	1008	—
$A_2'$ 3014	—	1415	1350	781	825	601	580
1224	—	1031	987	386	—	288	335
750	—	890	765				

a) Calculated by the use of the force constants listed in Table 1; in cm<sup>-1</sup> units.

b) Observed values<sup>2)</sup> in CS<sub>2</sub> and CCl<sub>4</sub> solutions or solid state. Essentially similar values are given in Refs. 3 and 4 for some of the frequencies.

c) The value calculated in Ref. 3, 60 cm<sup>-1</sup>, seems to be in error. See Ref. 1.

11) Y. Murata, K. Kuchitsu, and M. Kimura, *Japan. J. Appl. Phys.*, **9**, 591 (1970).

12) K. Kuchitsu, This Bulletin, **40**, 498 (1967).

13) Numerical experimental data of the levelled total intensity have been filed with the Chemical Society of Japan. A copy may be secured by citing the document number (Document No. 8002) and by remitting, in advance, ¥300 for photoprints. Payment may be made by check or money order payable to the Society.

14) Y. Morino, S. J. Cyvin, K. Kuchitsu, and T. Iijima, *J. Chem. Phys.*, **36**, 1109 (1962); K. Kuchitsu and S. Konaka, *ibid.*, **45**, 4342 (1966).

15) H. Takahashi and T. Shimanouchi, *J. Mol. Spectry.*, **13**, 43 (1964).

16) I. Suzuki, This Bulletin, **35**, 1279, 1449, 1456 (1962).

17) Y. Morino, K. Kuchitsu, and Y. Murata, *Acta Crystallogr.*, **18**, 549 (1965).

TABLE 4. CALCULATED CORRECTIONS FOR NONLINEAR SHRINKAGE EFFECTS FOR TRIETHYLENEDIAMINE<sup>a)</sup>

Set <sup>b)</sup>	I	II	III	IV	V
C <sub>2</sub> -C <sub>3</sub>	11	54	69	102	187
C <sub>2</sub> -C <sub>7</sub>	-4	17	24	40	80
C <sub>3</sub> -C <sub>7</sub>	-4	-11	-13	-18	-30
C <sub>2</sub> -N <sub>1</sub>	15	26	30	39	62
C <sub>3</sub> -N <sub>1</sub>	-1	5	8	13	26
N <sub>1</sub> -N <sub>4</sub>	-9	-9	-9	-9	-9
C-H	119	167	188	232	344
C <sub>2</sub> -H <sub>3a</sub>	48	134	168	239	423
C <sub>7</sub> -H <sub>2a</sub>	-27	16	29	60	143
C <sub>7</sub> -H <sub>3a</sub>	-18	-61	-78	-114	-208
C <sub>7</sub> -H <sub>2b</sub>	30	83	105	149	265
C <sub>7</sub> -H <sub>3b</sub>	28	43	50	63	97
N <sub>1</sub> -H <sub>7</sub>	55	104	125	167	276
N <sub>1</sub> -H <sub>8</sub>	16	38	46	63	108

a) Corrections  $r_a - r_\alpha$  (Ref. 14) calculated by using the force constants given in Table 1; in  $10^{-4}$  Å units. Corrections for the H-H pairs are omitted.

b) Sets I through V correspond to those in Table 3.

rium torsional angle  $\phi_e$  defined in Fig. 1. The dependence of the  $\phi_e$  parameters on  $Y$  was similar to that observed in the analysis of BO: By the use of  $Y=0.11$ , 0.08, and 0.05 md·Å, the cycles converged to nonzero sets ( $D_3$ ) of  $\phi_e$ ,  $9.8 \pm 1.1^\circ$ ,  $8.5 \pm 0.9^\circ$ , and  $5.4 \pm 3.0^\circ$  respectively, while  $\phi_e$  tended to  $0^\circ$  ( $D_{3h}$ ) for  $Y=0.025$  md·Å.

The situation that the alternative [twisted ( $D_3$ ) or untwisted ( $D_{3h}$ )] structures were derived from the analysis is in accordance with that encountered in the crystal-structure study of Weiss *et al.*,<sup>4)</sup> where the  $D_{3h}$  and  $D_3$  (with a twist angle of about  $10^\circ$  corresponding to  $\phi_e \sim 16^\circ$ ) structures, both reasonable answers of their three-dimensional X-ray analysis, made them suggest a double-minimum potential for the twisting motion. A similar trend observed in BO has been explained by a potential with a broad trough and shallow double minima.<sup>1)</sup> Therefore, TEDA is also expected to have a large-amplitude motion around the  $D_{3h}$  position, as is discussed below.

The rest of the independent parameters were unaffected by the choice of  $Y$ . The parameters obtained from the analysis are listed Table 5 with their limits of error (estimated as 2.5 times random errors plus systematic errors).<sup>17-19)</sup> The corresponding error matrix is given in Table 6. In contrast to the case of BO,

TABLE 5. STRUCTURAL PARAMETERS FOR TRIETHYLENEDIAMINE<sup>a)</sup>

N <sub>1</sub> -C <sub>2</sub>	$1.472 \pm 0.007$	$\angle$ N <sub>1</sub> -C <sub>2</sub> -C <sub>3</sub>	$110.2 \pm 0.4^\circ$
C <sub>2</sub> -C <sub>3</sub>	$1.562 \pm 0.009$	$\angle$ C <sub>2</sub> -N <sub>1</sub> -C <sub>7</sub>	$108.7 \pm 0.4^\circ$
C-H	$1.11_0 \pm 0.01_2$	$\angle$ H-C-H	$111.5 \pm 5.6^\circ$
$k^b)$	$0.97 \pm 0.04$		

a) Distances ( $r_g$ ) in Å and  $r_\alpha$  angles with estimated limits of error (See text).

b) Index of resolution (dimensionless).

18) K. Kuchitsu, T. Fukuyama, and Y. Morino, *J. Mol. Structure*, **1**, 463 (1968).

19) K. Kuchitsu, *This Bulletin*, **32**, 748 (1959).

TABLE 6. ERROR MATRIX<sup>a)</sup>

	C-N	C-C	C-H	$\angle$ N <sub>1</sub> -C <sub>2</sub> -C <sub>3</sub>	$\angle$ H-C-H	$\phi_e$	$k$
C-N	8	-6	-6	2	-17	10	-18
C-C		25	11	15	20	40	46
C-H			40	6	69	11	38
$\angle$ N <sub>1</sub> -C <sub>2</sub> -C <sub>3</sub>				20	33	-44	-13
$\angle$ H-C-H					316	-53	63
$\phi_e$						197	91
$k$							146

a) Error matrix for fixed mean amplitudes. Units ( $\times 10^{-4}$ ) for the distances are Å those for the angles are rad, and the index of resolution  $k$  is dimensionless. Elements of the matrix are given by  $\sigma_{ij} = \text{sgn}[(B^{-1})_{ij}] \cdot [|(B^{-1})_{ij}| \cdot V^*PV/(n-m)]^{1/2}$ , where the notations follow Ref. 20. The diagonal element  $\sigma_{ii}$  represents the standard error for the parameter  $i$ .

the analysis evidenced that none of the distance and angle parameters had strong correlation with the mean amplitudes. Therefore, it was further possible to treat a number of mean amplitudes as variable parameters in the least-squares calculations, from which the amplitudes listed in Table 7 were obtained, with no significant influence on the distance and angle parameters and their uncertainties given in Table 5.

TABLE 7. MEAN AMPLITUDES FOR TRIETHYLENEDIAMINE (in Å units)

	Obsd <sup>a)</sup>	Calcd <sup>b)</sup>
C-C	$0.051_8 \pm 0.004$	0.0519
C-N	$0.046_8 \pm 0.002$	0.0442
C-H	$0.076_4 \pm 0.002$	0.0781
C <sub>2</sub> -C <sub>7</sub>	$0.063_6 \pm 0.005$	0.0695
C <sub>3</sub> -C <sub>7</sub>	$0.083_4 \pm 0.009$	0.0877
C <sub>3</sub> -N <sub>1</sub>	$0.059_3 \pm 0.005$	0.0601
N <sub>1</sub> -H <sub>7</sub>	$0.110_6 \pm 0.007$	0.1014

a) Errors represent random standard deviations obtained by a least-squares analysis (see text).

b) Calculated by Set II of Table 3.

**Determination of the Potential Function.** The potential function for the twisting motion around the  $C_3$  symmetry axis, as characterized by a single torsional coordinate  $\phi$  illustrated in Fig. 1, was assumed to have a quadratic-quartic type,  $V(\phi) = k_2\phi^2 + k_4\phi^4$ . The molecular intensity function was averaged classically by the Boltzmann weight in regard to  $\phi$ . The coefficients of  $V(\phi)$  were determined by a least-squares method, by which the experimental molecular intensity was allowed to fit to the theoretical expression<sup>1)</sup> by the use of the mean amplitudes of set I given in Table 3. The most probable set was found to be  $k_2 = -5.5 \pm 4.2$  kcal/mol rad<sup>2</sup> and  $k_4 = 86.2 \pm 50.2$  kcal/mol rad<sup>4</sup>. The parameters specifying the potential shape are compared in Table 8 with those for BO.

The radial distribution curve corresponding to the best-fit potential is in good agreement with the experimental curve, as shown in Fig. 3, where a theoretical curve corresponding to a  $D_{3h}$  structure with small amplitudes of twisting and frame vibrations is also

20) K. Hedberg and M. Iwasaki, *Acta Crystallogr.*, **17**, 529 (1964).

TABLE 8. COMPARISON OF POTENTIAL PARAMETERS<sup>a)</sup>

	$k_2$	$k_4$	$V(0)^b)$	$\phi_e^c)$	$\phi_t^d)$	$\langle \phi^2 \rangle^{1/2e)}$
TEDA <sup>f)</sup>	$-5.5 \pm 4.2$	$86.2 \pm 50.2$	$87 \pm 100$	10	19.5	$11.0 \pm 1.5$
BO <sup>g)</sup>	$-4.0 \pm 3.3$	$54.2 \pm 34.5$	$75 \pm 100$	11	21.5	$12.0 \pm 1.5$
units	kcal/mol	kcal/mol	cal/mol	deg.	deg.	deg.

a) The twisting potential function,  $V(\phi) = k_2\phi^2 + k_4\phi^4$  ( $\phi$  in rad); errors for  $k_2$  and  $k_4$  represent standard deviations.

b) Potential hump at  $\phi = 0^\circ$ .

c) Potential minimum.

d) Classical turning point at  $20^\circ\text{C}$  (see Ref. 1).

e) Root-mean-square amplitude of twisting with limits of error estimated by a consideration of the correlation between the  $k_2$  and  $k_4$  parameters.<sup>21)</sup>

f) Triethylenediamine, determined in the present study (see text).

g) Bicyclo[2.2.2]octane (Ref. 1).

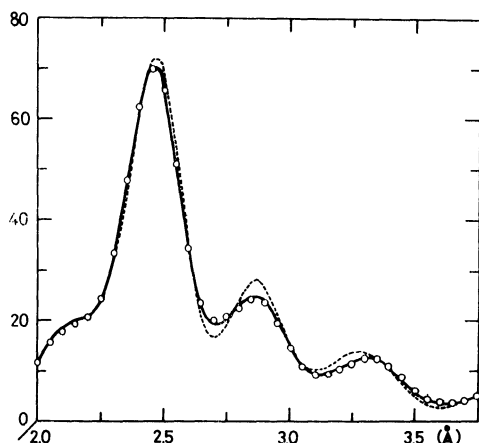


Fig. 3. Radial distribution curves for a region sensitive to the twisting motion.

Solid and broken lines represent synthetic curves calculated for the quadratic-quartic potential function  $V(\phi)$  determined in the text and for a quadratic function,  $V(\phi) = c\phi^2$  with  $c = 17$  kcal/mol rad<sup>2</sup>, corresponding to the force constant for torsion,  $Y = 0.08$  md·Å,<sup>21)</sup> respectively; circles represent experimental values and their estimated uncertainties.

displayed. The distinct peak at about  $2.8 \text{ \AA}$  is mainly composed of the nonbonded  $\text{C}_2\text{--C}_8$  and  $\text{C}_3\text{--C}_7$  pairs; a single sharp peak corresponding to a "rigid"  $D_{3h}$  conformation, where those pairs are equidistant, gets flattened as the system exerts a large-amplitude twisting motion. Thus, the contour of this peak offers a sensitive measure for the feature of the twisting potential.

## Discussion

**Structure.** The C–N bond distance,  $1.472 \pm 0.007 \text{ \AA}$ , is significantly longer than that of trimethylamine ( $1.451 \pm 0.003 \text{ \AA}$ )<sup>22)</sup> but is nearly equal to those of dimethylamine ( $1.466 \pm 0.005 \text{ \AA}$ ),<sup>23)</sup> methylamine ( $1.467 \pm 0.002 \text{ \AA}$ ),<sup>24)</sup> and ethylenediamine ( $1.468 \pm 0.005 \text{ \AA}$ ).<sup>25)</sup> The rest of the parameters are almost identical

with those for BO, as is contrasted in Table 9. The  $\text{C}_2\text{--C}_3$  bond length, which has been determined with a much higher accuracy than that of BO, is significantly (about  $0.02 \text{ \AA}$ ) longer than that of cyclohexane.<sup>26)</sup> A similar lengthening has recently been observed in the C–C distance of ethylenediamine.<sup>25)</sup> The C–C–N bond angle is found to be equal to that in ethylenediamine, both slightly larger than the tetrahedral angle. The bridgehead angle ( $\angle\text{C–N–C}$ ) is about  $2^\circ$  smaller than that in trimethylamine.<sup>22)</sup>

A good correspondence has been observed between the gas-phase and crystal structures of TEDA, as compared in Table 9. A similar correspondence reported in Ref. 1 between the free BO and a crystal-phase BO derivative<sup>27)</sup> suggests that the intramolecular geometrical parameters for such globular molecules are little influenced by intermolecular interactions, which should exist in the solid state.

**Potential Function.** From the potential function determined in Table 8, one sees that TEDA has a "quasi- $D_{3h}$ " structure analogous to that of BO (Fig. 4). Both molecules have potentials with double minima at  $\phi \sim 10^\circ$  and small humps at  $\phi = 0^\circ$ . In this connection,

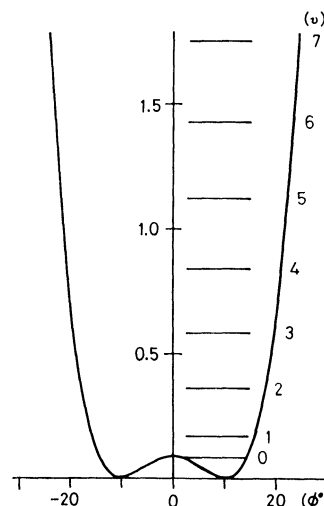


Fig. 4. The twisting potential function determined in terms of a torsional coordinate  $\phi$ ,  $V(\phi) = -5.5\phi^2 + 86.2\phi^4$  (kcal/mol); horizontal lines, calculated energy levels for this potential function (see text).

21) Y. Morino and T. Nakagawa, *J. Mol. Spectry.*, **26**, 496 (1968).

22) J. E. Wollrab and V. W. Laurie, *J. Chem. Phys.*, **51**, 1580 (1969).

23) J. E. Wollrab and V. W. Laurie, *ibid.*, **48**, 5058 (1968). See also B. Beagley and T. G. Hewitt, *Trans. Faraday Soc.*, **64**, 2561 (1968).

24) H. K. Higginbotham and L. S. Bartell, *J. Chem. Phys.*, **42**, 1131 (1965).

25) A. Yokozeki and K. Kuchitsu, *This Bulletin*, **43**, 2664 (1970).

26) H. Kambara, K. Kuchitsu, and Y. Morino, *ibid.*, to be published.

27) O. Ermer and J. D. Dunitz, *Helv. Chim. Acta*, **52**, 1861 (1969).

TABLE 9. COMPARISON OF THE STRUCTURES OF TRIETHYLENEDIAMINE AND RELATED COMPOUNDS

Molecule	TEDA		BO	EDA
	ED <sup>a)</sup>	XD <sup>b)</sup>	ED <sup>c)</sup>	ED <sup>d)</sup>
N-C <sup>e)</sup>	1.472	1.46±0.013 (1.46)	1.538±0.015	1.468±0.005
C-C	1.562	1.57±0.014 (1.54)	1.552±0.029	1.556±0.010
∠N-C-C <sup>e)</sup>	110.2°	110.0±1.0° (109.5°)	109.7±0.7°	110.2±0.8°
∠C-N-C <sup>e)</sup>	108.7°	108.9±0.8° (108.2°)	108.9±0.6°	—
C-H	1.110	—	1.107±0.009	—
∠H-C-H	111.5°	—	110.1±5.6°	—

TEDA; triethylenediamine, BO; bicyclo[2.2.2]octane, EDA, ethylenediamine, ED; electron diffraction, XD; X-ray diffraction. (Units; in Å for distances.)

a) Present study (See Table 5),  $r_g$  distances and  $r_a$  angles.

b) Crystal structure in Ref. 4. Values in parentheses represent the average structure of an acentric ( $D_3$ ) conformation with the twist angle of about 10°

c) Ref. 1,  $r_g$  distances and  $r_a$  angles.

d) Ref. 25,  $r_g$  distances and  $r_a$  angle.

e) For BO, the letter N should be replaced by C.

a similar potential for the 1-fluoro derivative of BO has recently been observed by Hirota from a microwave study.<sup>28)</sup>

The origin of the hump at  $D_{3h}$  may be explained by a semi-empirical calculation of strain energy, if plausible models can be estimated for nonbonded N-N and N-H interactions. One of the primitive approaches to this problem is to assume that the N-N and N-H interactions are equal to those for the C-C and C-H pairs, respectively. Such a calculation of the strain energy, analogous to that for BO, yielded a potential hump of about 130 cal/mol with double minima at  $\phi \sim 13.5^\circ$ , in reasonable agreement with the observed potential.

On the basis of the potential determined above, the energy levels for the twisting mode were estimated by the procedure described in Ref. 1. With an effective reduced mass of 26.8 amu calculated on the assumption of a semi-rigid framework, the levels given in Table 10 were obtained.

TABLE 10. ESTIMATED ENERGY LEVELS OF THE TWISTING MOTION FOR TRIETHYLENEDIAMINE<sup>a)</sup> ( $\text{cm}^{-1}$ ).

$v$	$E_v$	$v$	$E_v$	$v$	$E_v$
0	28.8	3	205.6	6	500.2
1	59.9	4	295.1	7	613.7
2	128.0	5	393.7	8	733.3

a) Semiquantitative estimates based on the experimental potential function,  $V = -5.5\phi^2 + 86.2\phi^4$  (kcal/mol,  $\phi$ ; in rad), determined in the present study.

## Appendix

*Construction of a High-Temperature Nozzle Assembly.* A nozzle assembly which can be heated to about 200°C was constructed for structure studies of compounds with vapor pressures less than several Torr at room temperature. The assembly, illustrated in Fig. 1a, may be classified into three parts: a) the nozzle body equipped with a heating pipe 4 and a cooling pipe 5 with water ducts 12, and a mechanism

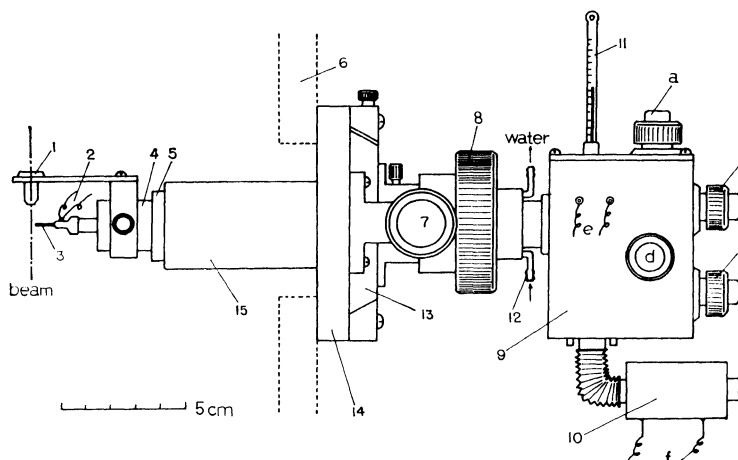


Fig. 1a. Nozzle assembly settled on a side-wall 6 of the diffraction chamber. The system is made vacuum-tight with metal O-ring contacts at 5—15, 13—14 (sliding) and 6—14 (fixed).

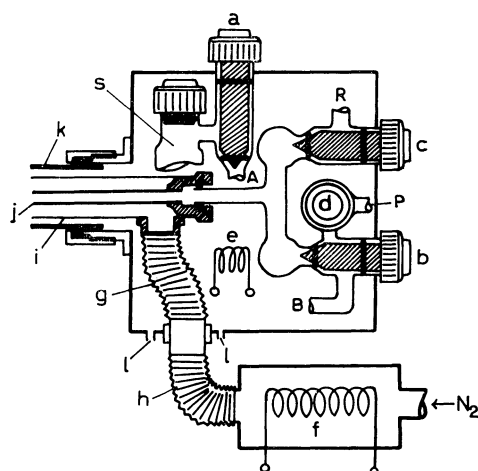


Fig. 2a. Inside section of the box 9 and the heater 10.

The walls are covered with asbestos. *a-d*: valves, *e, f*: electric heaters, *g-i*: paths of hot nitrogen gas, *j*: sample inlet, *k*: pipe corresponding to 4 in Fig. 1a, *l*: outlet of the nitrogen gas, *s*: sample holder with a connection *A, B* shown in Fig. 3a, *R*: reference gas inlet, *P*: outlet to a vacuum pump.

for adjustment 7, 8; *b*) an electric heater 10 supplying hot nitrogen gas as a thermal medium; *c*) valves *a-d* (Fig. 2a) and a sample holder (Fig. 3a) installed in a box 9.

The sample is heated to a required temperature in the sample holder. Valves *a* and *b* are then opened, and the sample vapor is allowed to flow through a horizontal stainless-steel pipe (3 mm inside diameter) in the heating pipe 4 and emit through a capillary 3 (0.2 mm i. d.) into the diffraction chamber, where it crosses the vertical electron beam at a preset distance (0.4–0.6 mm) from the nozzle tip and condenses on a trap cooled with liquid nitrogen.<sup>11)</sup>

Parts *b* and *c* are shown in Fig. 2a. The nitrogen gas heated by *f* (50Ω) flows through bellows *g* and *h* into a pipe *i*, heating the sample path *j*, and returns into the box, where the gas is again heated by *e* (125Ω) and ejected from the box (*l*) after heating the sample holder and the valves. At a normal flow rate of about 500 l·atm/min, and with A. C.

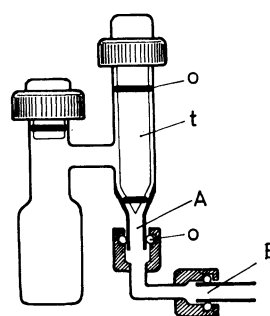


Fig. 3a. Cross section of the sample holder.

*A, B*: see corresponding parts in Fig. 2a, *o*: heat-resistant O-rings, *t*: teflon stopper.

voltages of 55 V applied on *f* and 25 V on *e*, the temperatures on the nozzle tip and inside the box reach 100°C. No disturbance on the electron beam caused by the heater currents is observed. The temperatures are measured with a copper-constantan thermocouple and a mercury thermometer, as shown in Fig. 1a. Thermal equilibrium is reached in several minutes, and a constant temperature (within  $\pm 1^\circ\text{C}$ ) can be maintained during the experiment (of the order of 10 min). The values (*a-d*) made of glass and teflon with heat-resistant O-rings are set up in the box: *a* and *b* for the sample, *c* for a reference gas, and *d* for an exhaust valve. The sample holder with valve *a* can be removed from the other parts in the box (at positions *A* and *B* in Fig. 3a) in order that the sample may be loaded or unloaded outside the box.

The nozzle assembly can be moved in two directions perpendicular to the electron beam so as to make the beam pass through the aperture 1<sup>11)</sup> by means of ball-bearing systems 7, 8 and sliding systems 13–15 with O-rings shown in Fig. 1a. The changes in the camera length by this adjustment and by thermal strain are found to be within 0.01 mm. The camera length is first estimated by a cathetometer and is later determined by the analysis of a diffraction pattern for a standard sample ( $\text{CO}_2$  or  $\text{N}_2$ ), which can be introduced into the diffraction chamber by the use of valve *c* in place of the sample to be studied at an identical experimental condition. In this way, the scale factor can be calibrated to within 0.07%.